ELECTRONIC SUPPLEMENTARY INFORMATION

Surface Core Level BE Shifts for CaO(100): Insights Into Physical Origins

Paul S. Bagus[1], Connie J. Nelin[2], Sergey Levchenko[3,4], and Xunhua Zhao[3,5],
Earl M. Davis[6], Helmut Kuhlenbeck[6], and Hans-Joachim Freund[6]

[1] *Department of Chemistry, University of North Texas, Denton, Texas 76203-5017, USA*
[2] *6008 Maury's Trail, Austin, Texas 78730, USA*
[3] *Abteilung Theorie, Fritz-Haber-Institut der Max-Planck-Gesellschaft, Faradayweg 4-6, D-14195 Berlin, Germany*
[4] *Current address: Skolkovo Institute of Science and Technology, Skolkovo Innovation Center, 3 Nobel Street, 143026 Moscow, Russia*
[5] *Current address: Department of Physics, University of Texas, Austin, Texas, 78712, USA*
[6] *Abteilung Chemische Physik, Fritz-Haber-Institut der Max-Planck-Gesellschaft, Faradayweg 4-6, D-14195 Berlin, Germany*

I. Considerations for Experimental Procedures and Results.

Core level XPS measurements were performed using a PHOIBOS 100 2D-CCD hemispherical analyzer from SPECS GmbH. The apparatus consisted of two chambers - a preparation chamber containing facilities for sample preparation and characterization, and an analysis chamber where the XPS measurements were performed. For sample preparation and film growth, a quartz microbalance for film thickness calibration, a Ca evaporator, a gas dosing system, a tungsten filament for sample heating, a sputter gun and a LEED system for checking the quality and the order of prepared surfaces were all available in the preparation chamber. The base pressure of the two chambers was 1×10^{-10} mbar and 4×10^{-11} mbar, respectively.

The CaO(100) films were prepared on a Pt(100) single crystal cleaned by cycles of Ar^+ ion sputtering, oxidation, and annealing until a sharp LEED pattern of the (5 × 20) reconstruction [1] was observed. Well-ordered CaO films were then prepared by depositing Ca from the evaporator at a rate of 20 Å/min in an oxygen partial pressure of 1×10^{-6} mbar at room temperature, followed by annealing the sample for 5 minutes at 1045 K in 5×10^{-7} mbar O_2 and then for 5 minutes at 1075 K in 2×10^{-7} mbar O_2 until a well-ordered surface was achieved as judged by LEED, Fig. S1. This procedure resulted in films with a thickness of approximately 11 nm. Due to the reactivity of CaO surfaces with typical residual gases found in UHV systems, prior to measurement the sample was flashed to 975 K in the preparation chamber and transferred to the analysis chamber while still hot in order to avoid the formation of hydroxyls at the surface. A small amount of Pt was observed to have migrated into the film (approx. 5% concentration within film) following annealing of the sample at 1075 K. However, for less-well-ordered samples, annealed at 1015 K and without migration of Pt, the same core level shifts were observed which leads us to the conclusion that the Pt contamination did not affect the SCLS. In these cases, due to the increased disorder, the intensity of the surface core level peak was reduced.

Ca 2p photoemission spectra were obtained using various photon energies. For the photon energy of 750 eV, the photoelectron kinetic energy is ≈350 eV and for hν = 450 eV, the photoelectron kinetic energy is ≈100 eV. The IMFP, inelastic mean free electron path, as calculated using the QUASES-IMFP-TPP2M software [2] decreases from 10.2 Å to 5.4 Å between these photon energies showing the greater surface sensitivity for hν = 450 eV. For the photon energies for the O 1s spectra shown in Fig. 3 of the main text, the photoelectron IMFP's were varied from 4.8 Å to 8.6 Å by variation of the photon energy from 600 to 800 eV.

II. Theoretical Methods and Calculations

The logic for the choices of cluster size and composition follow considerations originally developed to describe vibrational excitations in the XPS [3]where large clusters had to be used to properly take into account the compressional effects of the extended ions of the solid. [4] The main features are: (1) The central atom of the cluster is the atom for which the core-level BEs are determined. This atom is surrounded by shells of neighboring anions and cations to represent the environment of the ionized atom. The surroundings are chosen so that the edge atoms of the cluster are Ca cations rather than O anions. The Ca cations, as is shown in the results, are reasonably rigid while the O anions are more deformable. An important function of the Ca cations at the edges of the clusters is to compress the charges associated with the O anions and not allow them to expand; thus, the edge Ca cations have a compressional effect on the O anions. [4] For clusters that model the bulk, all the O anions in the clusters have 6 nearest neighbor Ca cations while the edge Ca cations have some nearest neighbor O anions and some nearest neighbor point charges. The point charges which are included to represent the Madelung potential of the extended CaO crystal are chosen following the Evjen procedure [5] where the point charges for the bulk have values of the nominal ionicity, +2 or −2, while surface, edge and corner point charges have fractional charges. For the clusters to model the bulk, more than 500 point charges were used and they provide an accurate description of the Madelung potential. The atoms and point charges are placed at lattice sites for bulk CaO. [6] The cluster models of the CaO(100) surface are formed by truncating the cluster models for the bulk.

The localization of the orbital of the ionized core electron is a natural consequence of the construction of the clusters. This is because the ionized atom is the central atom of the cluster and this atom is inequivalent to the other atoms in the cluster. Thus, both the initial and final, ionized, state central atom core orbitals are localized.

The CSOV has been used to determine the energetic importance of covalent interactions in CaO. The aspects specific to the use of the CSOV for CaO are as follows: The Ca^{2+} and embedded

O_6Ca_{18} fragments are used for the CSOV analysis of the covalent bonding for the embedded CaO_6Ca_{18} cluster. In the first step of the CSOV, the isolated Ca^{2+} and the O_6Ca_{18} cluster are superimposed. The Ca^{2+} orbitals are frozen and the O_6Ca_{18} fragment orbitals are optimized but the central Ca occupied and virtual orbitals are removed from the variational process. This step allows the O_6Ca_{18} fragment orbitals to adjust to the presence of the spatially extended charge distribution of the central Ca^{2+} cation. In a following step, the O_6Ca_{18} orbitals are frozen and the Ca^{2+} orbitals are optimized but only in the space of the Ca occupied and virtual orbitals. These two steps represent ideal ionic interactions. Further CSOV steps: (1) Allow the Ca^{2+} orbitals to be varied with the embedded O_6Ca_{18} fragment frozen but including in the variational space the virtual orbitals of the O_6Ca_{18} fragment. And (2) allow the O_6Ca_{18} fragment orbitals to be varied with the Ca fragment orbitals frozen but including in the variational space the virtual orbitals of the Ca^{2+} fragment. These later two steps represent departures from ideal ionic interactions. They provide a compliment to confirm the analysis of the ionicity obtained with the orbital projections.

The HF calculations were carried out using an extended basis set which is of double zeta quality for the core orbitals and better than double zeta for the valence orbitals. For most of the Ca atoms, basis functions were included to represent the Ca 3d orbital although no evidence is found that this orbital is involved in covalent bonding of Ca with O; these d basis functions were not included for the edge Ca toms of the $OCa_6O_{18}Ca_{38}$ cluster. For most of the O atoms a d polarization function was included, although not for the outer O atoms of the $OCa_6O_{18}Ca_{38}$ cluster. The spatial parts of the spin up and spin down orbitals for each shell or sub-shell are restricted to be the same in all the initial and final state wavefunctions. The calculations for the WFs and the analysis were performed with the CLIPS suite of programs. [7]

III. Analysis of the Covalent Bonding in CaO

The projections indicate that for CaO, there is a small contribution of a covalent bonding to the interaction. This minor covalent bonding would have to be with the Ca 3d orbitals since the sizes of the Ca 4s and 4p are too large to allow covalent bonding with O(2p). The CSOV estimate of 0.7 eV for the contribution of the covalent interaction includes a correction for the limitations of the basis sets used to describe the O and Ca ions. Without this correction, the energy improvement by allowing the orbitals of the O anions to mix with the unoccupied orbitals of the Ca^{2+} cation is 0.80 eV. However, a part of this energy improvement may come because the Ca orbitals are used to improve the description of the O anions, a process which is described as basis set superposition. [8] The basis set superposition can be estimated by calculating the energy of the fragment containing the oxygen anions in a basis that contains the functions of the central Ca atom; in particular, the unoccupied orbitals of Ca^{2+}. This estimate indicates that the superposition accounts for only 0.13 eV of the energy improvement. Thus, the covalent bonding leads to a contribution of ~0.7 eV to interaction

IV. Density Difference Plots of Core-Hole Relaxation

The relaxation in response to the core holes in CaO can be viewed graphically with density difference plots where the density of the ground state wavefunction is subtracted from the relaxed density of core-ion wavefunction. The density difference, $\Delta\rho$, is defined as $\Delta\rho = \rho(\text{core-ion}) - \rho(\text{initial state})$ where $\Delta\rho>0$ is when the relaxation increases the density and $\Delta\rho<0$ is when the density has been decreased. The $\Delta\rho$ for bulk and surface Ca 2p ions are given in Fig. S2 and for the O 1s ions in Fig. S3. These plots were made with the Mahler programs developed by K. Hermann. [9] For the Ca 2p, the plots are for the average ρ for removal of an electron from each of the three 2p orbitals. The plots are in a plane and show the contours of constant density difference in this plane as either solid lines, "−−−−", for $\Delta\rho>0$ or dashed lines, "− − − −", for $\Delta\rho<0$; the contours for $\Delta\rho=0$ are shown with short dashes, '- - - -'. The contours are for values of Δρ that change by increments of Δ_{step} about the $\rho=0$ contours. The contours are only shown for $|\Delta\rho|$ less than a maximum value to minimize regions where there will be a large density of contours. For all plots, the ionized atom is at the center. The plane of the plots for the bulk Δρ, Figs. S2(a) and S3(a), is parallel to the (100) surface and contains four of the nearest neighbor counter ions of the central ionized atom. Two planes are considered for the surface ions: the plotting planes for Figs. S2(b) and S3(b) are in the (100) surface while the planes of Figs. S2(c) and S3(c) are normal to the (100) surface plane and contain three of the nearest neighbor counter ions of the central ionized atom, two in the surface plane and one in the second layer of CaO. The positions of the atomic centers in the plotting planes are shown in the figures.

For the relaxation for the bulk Ca 2p ion, Fig. S2(a), there is a large contraction of the Ca^{2+} charge toward the Ca nucleus in response to the removal of a Ca 2p electron as shown by the charge reduction inside the first contour of $\Delta\rho=0$ around the central Ca atom because the outer orbitals of the Ca 2p ion are contracted toward the center of the Ca region. This is consistent with a large atomic relaxation energy of 10.19 eV, see Table II of the main text. There is a modest polarization of the O anion charge toward the Ca anion with a 2p-hole as can be seen by the two contours of $\Delta\rho>0$ between the Ca and the O neighbors as well as the reduction in charge directly around the O anions. It is this polarization of the O charge that leads to the extra-atomic relaxation energy of 2.55 eV, see Table II of the main text, since the polarization of the next nearest Ca cations is seen, Fig. S2(a), to be quite small. For the surface Ca 2p ion, the relaxation in the surface plane, Fig. S2(b), is almost identical to that around the bulk Ca 2p ion, Fig. S2(a). The relaxation normal to the surface, Fig. S2(c) has minor differences from that in the surface plane. The main change is that the Ca relaxation above the surface extends further from the Ca center than it does in the plane; this is because the sixth O neighbor above the (100) surface is missing and does not provide the compression of the Ca charge [4, 10] that is present in the (100) surface and in the bulk. In other words, even for the rigid Ca^{2+} cations, the surface cations have some differences from those in the bulk.

In a similar way as for the Ca(2p) ionization, the $\Delta\rho$ for the bulk O(1s) ionization, Fig. S3(a), involves contraction of the outer O 2s and 2p orbitals toward the O nucleus in response to an effective increase of the O nuclear charge from 8 to 9. [11-12] This is seen from the large series of $\Delta\rho<0$ contours around the central O nucleus. There is also polarization of the charges of the surrounding atoms toward the core-ionized O atom as can be seen by the contours of $\Delta\rho>0$ between the central O and the nearest neighbor Ca atoms indicating some polarizability of the Ca^{+2} cations. However, there is also a modest polarization of the more distant O anions, those at the edges of the contour plot as shown by several contours of $\Delta\rho<0$ around these atoms. The polarization of these more distant atoms in response to an O(1s) ion is in sharp contrast to the much more minor polarization of the equivalent, more distant, Ca atoms; see Fig. S2(a). This difference between the polarization in response to the Ca 2p ionization and the O 1s ionization reflects the much larger polarizability of O^{-2} than Ca^{+2}. For the surface O(1s) relaxation within the CaO(100) surface, Fig. S3(b), the $\Delta\rho$ contours are similar to those for the bulk O(1s), Fig. S3(a). The $\Delta\rho$ contours in the plane normal to CaO(100) show similar contraction of the central, 1s ionized O as well as similar polarizations of the charge of the neighboring Ca and O atoms. Just as was the case for the relaxation about a 2p-hole in a surface Ca, the relaxation above the ionized surface O is larger than within the surface or in the bulk reflecting the absence of the compression of the missing Ca cation above the surface O anion.

Overall, the information from the Δρ plots in Figs. S2 and S3 is consistent with the atomic and extra-atomic relaxations given in Table II. The total relaxation energy in response to the 1s ionization of a bulk O atom is 22.7 eV, or about twice as large as for the 2p ionization of a bulk Ca atom and a very large fraction of the increase in E(R) is due to a larger atomic relaxation for the O anion. Furthermore, the smaller extra-atomic relaxation for the bulk O(1s) than for bulk Ca(2p) is consistent with the different polarizations shown in Figs. S2(a) and S3(a).

V. SCLS For Ionization of the Surface Ca 2pσ and 2pπ Orbitals

The surface Ca 2p orbitals are the nearly degenerate 2pσ and 2pπ orbitals. The surface 2p ionization can be for the removal of either a 2pσ, normal to the CaO(100) surface, a 2pπ, parallel to the surface or an average ionization, 2p(Avg). The WF for 2p(AVG) is for an occupation of 1/3 of a hole in the surface Ca(2pσ) and 2/3 of a hole in the surface Ca(2pπ). The SCLS(KT) and SCLS(ΔSCF) for these different surface ionizations are given in Table SI. Since, the variational calculations for the surface 2pσ, 2pπ, and 2p(AVG) BEs are for different occupations of the 2pσ and 2pπ orbitals, the SCLS(ΔSCF) for 2p(AVG) is not exactly the weighted average of the 2pσ and 2pπ SCLS(ΔSCF). The different Ca 2p SCLS values are essentially identical indicating that the initial and final state effects are independent of the 2p orbital ionized.

References

1. H. P. Bonzel, C. R. Helms, and S. Kelemen, "Observation of a Change in the Surface Electronic Structure of Pt(100) Induced by Reconstruction", Phys. Rev. Lett. **35**, 1237 (1975).
2. http://www.quases.com/products/quases-imfp-tpp2m/.
3. C. J. Nelin *et al.*, "Analysis of the Broadening of X-ray Photoelectron Spectroscopy Peaks for Ionic Crystals", Angew. Chem. Int. Ed. **50**, 10174 (2011).
4. J. Q. Broughton and P. S. Bagus, "Self-consistent-field studies of core-level shifts in ionic crystals. II. MgO and BeO", Phys. Rev. B **36**, 2813 (1987).
5. H. M. Evjen, "On The Stability of Certain Heteropolar Crystals", Phys. Rev. **39**, 675 (1932).
6. R. W. G. Wyckoff, *Crystal Structures* (Wiley, New York, 1963).
7. *CLIPS is a program system to compute ab initio SCF and correlated wavefunctions for polyatomic systems. It has been developed based on the publicly available programs in the ALCHEMY package from the IBM San Jose Research Laboratory by P. S. Bagus, B. Liu, A. D. McLean, and M. Yoshimine.*
8. S. F. Boys and F. Bernardi, "The calculation of small molecular interactions by the differences of separate total energies. Some procedures with reduced errors", Mol. Phys. **19**, 553 (1970).
9. K. Hermann, *available as plotting utility KHPLTPS of the Stobe package, see* http://www.fhi-berlin.mpg.de/KHsoftware/StoBe/StoBeMAN.html#2.7.3.
10. C. J. Nelin *et al.*, "Surface core-level binding energy shifts for MgO(100)", Phys. Chem. Chem. Phys. **16**, 21953 (2014).
11. J. W. Koepke and W. L. Jolly, "The core electron binding energies of oxygen difluoride", J. Electron Spectrosc. Relat. Phenom. **9**, 413 (1976).
12. W. L. Jolly, "The estimation of core-electron binding-energy shifts using the concept of the equivalence of equally charged cores", in *Proceedings of the international conference on electron spectroscopy*, edited by D. A. Shirley (North-Holland, Amsterdam, Netherlands, 1972), p. 629.

Table SI. Initial state and final state Ca 2p SCLS, in eV, in CaO for the ionization of different surface 2p electrons, 2pσ, 2pπ, and 2p(Avg).

		SCLS(KT)	SCLS(ΔSCF)
Ca	2p(Avg)	0.89	1.01
	2pπ	0.89	1.00
	2pσ	0.90	1.00

Figure S1: LEED image, taken with 70 eV electrons, of a CaO(100) film annealed at 1075 K.

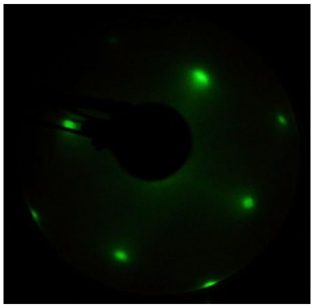

Fig. S2. Electron density difference plots for (a) bulk Ca 2p ionization and (b) and (c) surface Ca 2p ionization. The position of the central Ca cation is shown as a blue circle, online, and of the immediate O anion neighbors are shown as green, online, circles. For the bulk (a) and the surface plane, (b) there are four nearest neighbors while for the plane normal to the surface, (c) there are only three nearest neighbors, two in the surface layer and one in the layer below the surface. Solid lines indicate an increase of density in response to the core-hole on the central ion and short dashed lines indicate a decrease of density due to this relaxation. See text for a complete description of the contours and plotting planes.

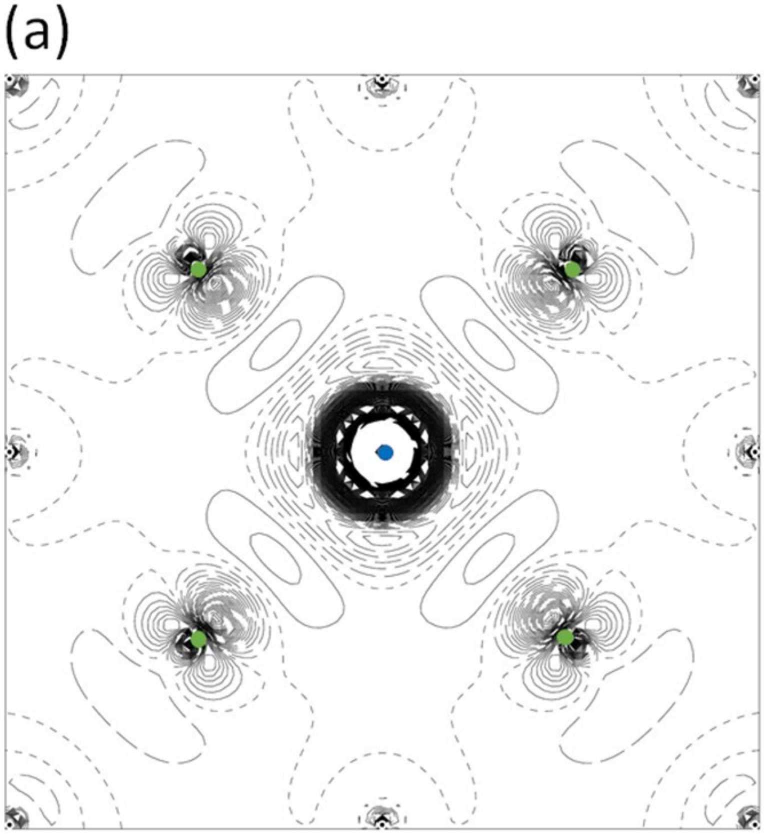

(b)

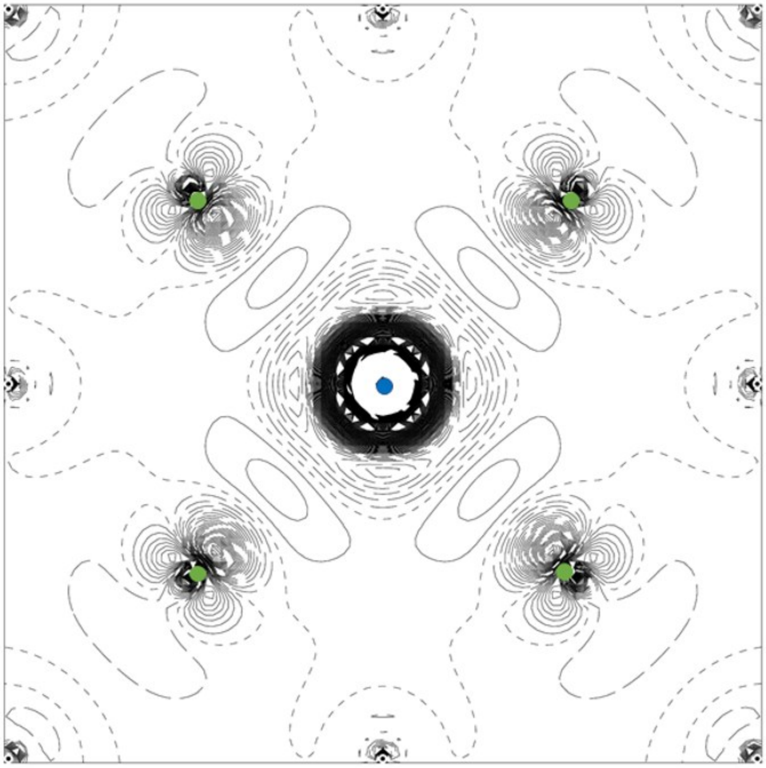

(c)

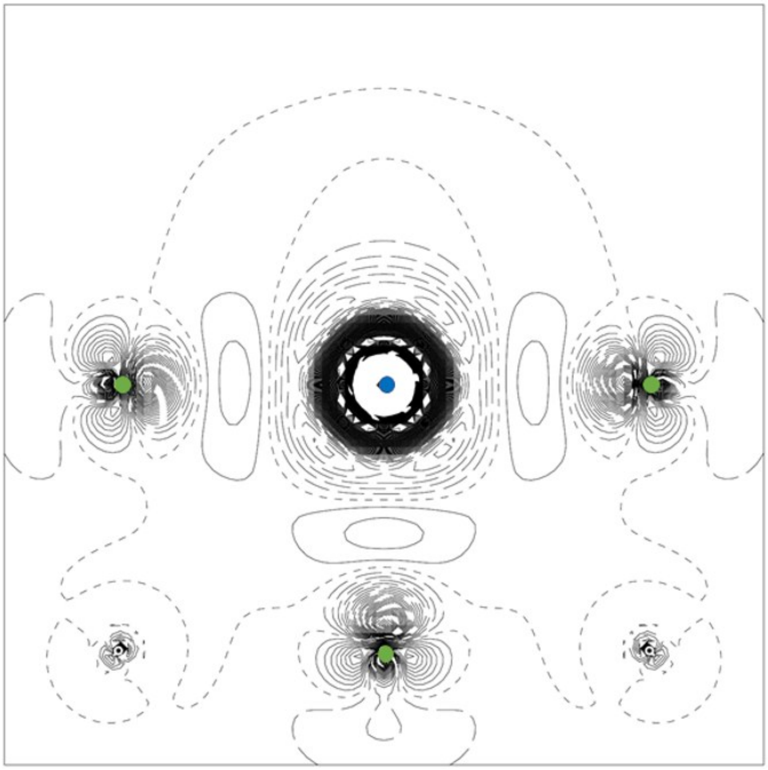

Fig. S3. Electron density difference plots for (a) bulk O 1s ionization and (b) and (c) surface O 1s ionization; the positions of the atomic centers are shown in the figures; see text and caption to Fig. S1.

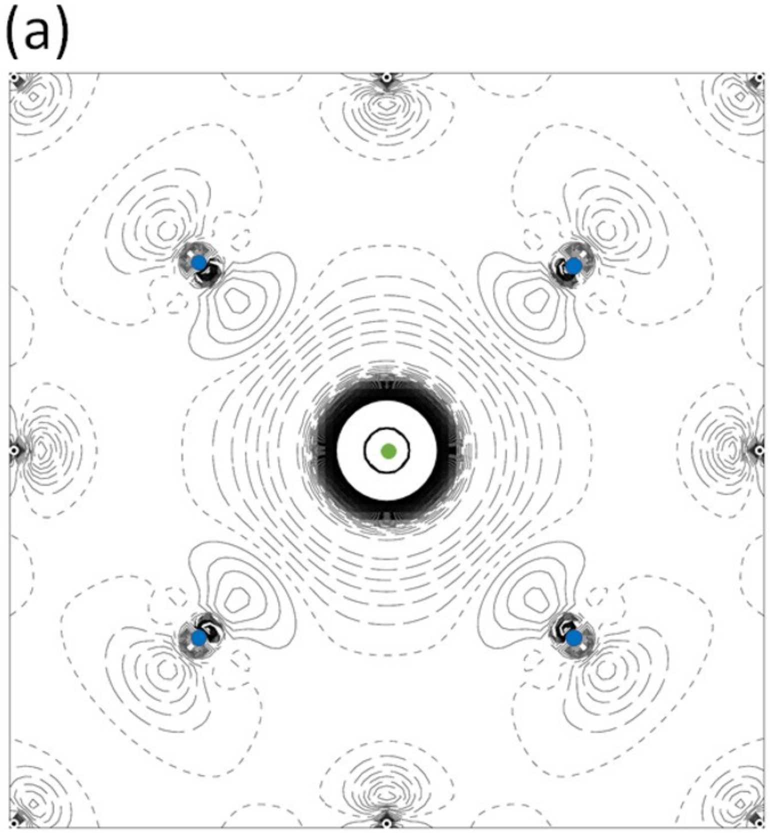

(b)

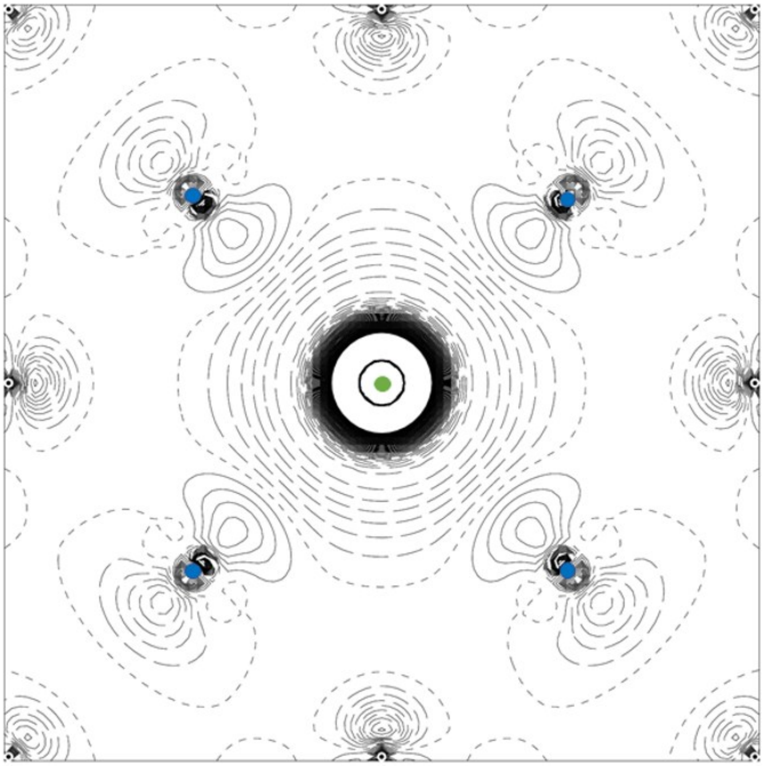

(c)